Decreased SPTBN2 expression regulated by the ceRNA network is associated with poor prognosis and immune infiltration in low-grade glioma

GUO-RONG CHEN[1,2*], YI-BIN ZHANG[1,2*], SHU-FA ZHENG[1,2*], YA-WEN XU[1,2], PENG LIN[3], HUANG-CHENG SHANG-GUAN[1,2], YUAN-XIANG LIN[1,4], DE-ZHI KANG[1,2,4-6] and PEI-SEN YAO[1,2]

[1]Department of Neurosurgery, Neurosurgical Research Institute, The First Affiliated Hospital, Fujian Medical University, Fuzhou, Fujian 350005; [2]Department of Neurosurgery, National Regional Medical Center, Binhai Campus of The First Affiliated Hospital, Fujian Medical University, Fuzhou, Fujian 350212; [3]Department of Pain; [4]Fujian Key Laboratory of Precision Medicine for Cancer; [5]Key Laboratory of Radiation Biology of Fujian Higher Education Institutions; [6]Fujian Provincial Institutes of Brain Disorders and Brain Sciences, The First Affiliated Hospital, Fujian Medical University, Fuzhou, Fujian 350005, P.R. China

Received August 16, 2022; Accepted February 24, 2023

DOI: 10.3892/etm.2023.11952

Abstract. The majority of low-grade gliomas (LGGs) in adults invariably progress to glioblastoma over time. Spectrin β non-erythrocytic 2 (*SPTBN2*) is detected in numerous tumors and is involved in tumor occurrence and metastasis. However, the specific roles and detailed mechanisms of *SPTBN2* in LGG are largely unknown. The present study performed pan-cancer analysis for the expression and prognosis of SPTBN2 in LGG using The Cancer Genome Atlas and The Genotype-Tissue Expression. Western blotting was used to detect the amount of SPTBN2 between glioma tissues and normal brain tissues. Subsequently, based on expression, prognosis, correlation and immune infiltration, non-coding RNAs (ncRNAs) were identified that regulated *SPTBN2* expression. Finally, tumor immune infiltrates associated with *SPTBN2* and prognosis were performed. Lower expression of *SPTBN2* was correlated with an unfavorable outcome in LGG. A significant correlation between the low *SPTBN2* mRNA expression and poor clinicopathological features was observed, including wild-type isocitrate dehydrogenase status (P<0.001), 1p/19q non-codeletion (P<0.001) and elders (P=0.019). The western blotting results revealed that, compared with normal brain tissues, the amount of SPTBN2 was significantly lower in LGG tissues (P=0.0266). Higher expression of five microRNAs (miRs/miRNAs), including *hsa-miR-15a-5p, hsa-miR-15b-5p, hsa-miR-16-5p, hsa-miR-34c-5p* and *hsa-miR-424-5p*, correlated with poor prognosis by targeting SPTBN2 in LGG. Subsequently, four long ncRNAs (lncRNAs) [*ARMCX5-GPRASP2, BASP1*-antisense RNA 1 *(AS1), EPB41L4A-AS1 and LINC00641*] were observed in the regulation of *SPTBN2* via five miRNAs. Moreover, the expression of *SPTBN2* was significantly correlated with tumor immune infiltration, immune checkpoint expression and biomarkers of immune cells. In conclusion, *SPTBN2* was lowly expressed and correlated with an unfavorable prognosis in LGG. A total of six miRNAs and four lncRNAs were identified as being able to modulate *SPTBN2* in a lncRNA-miRNA-mRNA network of LGG. Furthermore, the current findings also indicated that SPTBN2 possessed anti-tumor roles by regulating tumor immune infiltration and immune checkpoint expression.

Introduction

Throughout the last 10 years, glioma has persisted as the foremost prevalent and lethal primary brain tumor among adult populations worldwide, exhibiting an annual incidence of 6 cases per 100,000 individuals and a 5-year overall survival rate not exceeding 35% (1,2). According to recent studies, low-grade gliomas (LGG) account for 15-20% of all adult gliomas and correlate with a median overall survival of 10 years, which is higher compared with the median overall survival of high-grade glioma (HGG) (3,4). Tumor-associated epilepsy is a common symptom in patients with LGG (5). Nevertheless, patients with LGG have a higher mortality rate when compared with the general population (6). Despite improved advancements in diagnostics and therapeutic techniques, the majority of LGGs in adults invariably progress to glioblastoma (GBM) over time (7). Moreover, high-risk LGG patients display shorter survival outcomes when compared

Correspondence to: Professor De-Zhi Kang or Dr Pei-Sen Yao, Department of Neurosurgery, Neurosurgical Research Institute, The First Affiliated Hospital, Fujian Medical University, 20 Chazhong Road, Taijiang, Fuzhou, Fujian 350005, P.R. China
E-mail: kdz99988@vip.sina.com
E-mail: peisen_yao@fjmu.edu.cn

*Contributed equally

Key words: spectrin β non-erythrocytic 2, ceRNA network, low-grade glioma, immune infiltration, outcome

with low-risk LGG patients (8,9). Thus, it is necessary to elucidate the prognostic predictors and underlying molecular mechanisms in patients with LGG.

Spectrin β non-erythrocytic 2 (*SPTBN2*), also termed β-III spectrin, is highly expressed in the brain and plays an important role in the neuronal membrane skeleton (10). SPTBN2 regulates glutamate-associated pathways by stabilizing excitatory amino-acid transporter 4 (11). *SPTBN2* is detected in numerous tumors and is involved in tumor occurrence and metastasis (12-14). The expression of *SPTBN2* is higher in lung cancer compared with in normal lung tissues (14). In addition, *SPTBN2* expression is correlated with the prognosis of patients with lung adenocarcinoma (14). *SPTBN2* is significantly overexpressed in endometrioid endometrial cancer and is positively associated with poor prognosis (15).

The *SPTBN2* expression, prognosis and regulatory mechanism in LGG remain elusive. A prior study revealed that *SPTBN2* has an adverse effect on reduced infiltration of $CD4^+$ T cells, contributing to a suboptimal prognosis for patients with ovarian cancer (16). Nevertheless, the potential function of *SPTBN2* in regulating tumor immune infiltration in LGG is poorly understood. The present study performed expression and survival analyses for *SPTBN2* in a pan-cancer study. Next, the potential upstream noncoding RNAs (ncRNAs) of *SPTBN2* were investigated in LGG, including microRNAs (miRNAs/miRs) and long noncoding RNAs (lncRNAs). Finally, the relationship of *SPTBN2* expression to immune infiltration, immune biomarkers, and immune checkpoints in LGG was determined. The aim of the present study was to investigate the association between ncRNA-mediated downregulation of SPTBN2 and tumor immune infiltration and prognosis in patients with LGG.

Materials and methods

Ethics approval and consent to participate. The study was approved by the Ethics Committee of the First Affiliated Hospital of Fujian Medical University (approval no. MRCTA, ECFAH of FMU [2022]509).

The Cancer Genome Atlas (TCGA) data download, process, and analysis. Pan-cancer gene expression data were obtained from TCGA database (https://tcga-data.nci.nih.gov/tcga/; V33.0; accession no. phs001145). The 33 TCGA cancer types analyzed are presented in Table SI. A differential expression analysis of *SPTBN2* was performed using the R package (version 3.6.3) (17). Weighted Pearson correlations and P-values were also calculated using the R package (version 3.6.3) 'weights' (https://CRAN.R-project.org/package=weights) (18). $P<0.05$ was considered to indicate a statistically significant difference. The clinicopathological features of patients with LGG are displayed in Table I. Patients with incomplete clinical information were excluded.

Gene Expression Profiling Interactive Analysis (GEPIA) database analysis. GEPIA (http://gepia.cancer-pku.cn/detail.php; accessed on 16 August 2022; accession no. GEPIA2) is a web server for gene-expression profiling and correlation analysis based on The Genotype-Tissue Expression (GTEx) data and TCGA (19). GEPIA was used to analyze *SPTBN2* and lncRNA expression in various types of cancer. An appropriate expression threshold was selected to split the high and low expression cohorts by grouping cut-offs. High cut-off values were considered to be samples with expression levels above this threshold, and were the high expression cohorts. Samples with lower cut-off values were considered to have an expression level below this threshold and were considered to be the low-expression cohort. A comparison of high and low-expression groups was completed using GEPIA. $P<0.05$ was considered to indicate a statistically significant difference. GEPIA was used to generate survival analysis for *SPTBN2* pan-cancer studies, including overall survival (OS) and disease-free survival (DFS). Also, candidate lncRNAs in *SPTBN2* were assessed prognostically using GEPIA. Cluster of differentiation 274 (*CD274*), programmed cell death 1 (*PDCD1*), cytotoxic T lymphocyte antigen 4 (*CTLA4*), sialic acid-binding immunoglobulin-like lectin 15 (*SIGLEC15*), T cell immunoreceptor with Ig and immunoreceptor tyrosine-based inhibitory domains (*TIGIT*), hepatitis A virus cellular receptor 2 (*HAVCR2*), lymphocyte activation gene-3 (*LAG3*), indoleamine 2,3-dioxygenase 1 (*IDO1*) and programmed cell death 1 ligand 2 (*PDCD1LG2*) were selected to be immune checkpoints. The GEPIA database investigated the relationship between SPTBN2 and immune checkpoints in LGG.

Encyclopedia of RNA Interactomes (ENCORI) database analysis. ENCORI (http://starbase.sysu.edu.cn/; accessed on 16 August 2022, version 2.0) is an online publicly accessed platform for studying the interactions between various RNAs (20). Candidate miRNAs were generated using ENCORI. Several target prediction programs were used to obtain upstream binding miRNAs of *SPTBN2*, including RNA22, PITA, miRmap, microT, PicTar, miRanda and TargetScan (http://starbase.sysu.edu.cn; version 2.0) (21). In addition, parameters for degradome data (low stringency) and pan-cancer type (one cancer type) were set. Only the predicted miRNAs obtained in at least three programs were considered candidate miRNAs of *SPTBN2* and included for subsequent analysis. ENCORI was also used to generate the correlation between miRNAs and *SPTBN2* in LGG. miRNAs negatively correlated with SPTBN2 were selected for subsequent survival analysis. Survival analysis of candidate miRNAs was performed by the ggplot2 R package (version 3.6.3) (https://cran.r-project.org/package=ggplot2) (22). Besides, candidate lncRNAs that could potentially bind to candidate miRNAs were generated using ENCORI.

Prediction of lncRNA and ceRNA network construction. Analysis of miRNet2.0 (www.mirnet.ca/miRNet/home.xhtml; version Primeface 11) and ENCORI was implemented to predict targeted lncRNAs of miRNAs. The positive correlation between *SPTBN2* and targeted lncRNAs was analyzed using miRNet2.0 databases following the ceRNA hypothesis. Moreover, a lncRNA-miRNA-mRNA interaction network of *SPTBN2* was constructed using ENCORI to understand post-transcriptional gene regulation. Overall survival analysis of these candidate miRNAs was performed using R package. The Sankey diagram was generated using SankeyMATIC (www.sankymatic.com).

Table I. Correlation of SPTBN2 mRNA with clinicopathological features in The Cancer Genome Atlas cohort.

Characteristic	Low expression of SPTBN2	High expression of SPTBN2	P-value[a]
Total, n	264	264	
WHO grade, n (%)[a]			0.204
Grade 2	102 (21.8)	122 (26.1)	
Grade 3	126 (27.0)	117 (25.1)	
IDH status, n (%)[a]			<0.001
WT	76 (14.5)	21 (4.0)	
Mut	187 (35.6)	241 (45.9)	
1p/19q codeletion, n (%)[a]			<0.001
Codel	54 (10.2)	117 (22.2)	
Non-codel	210 (39.8)	147 (27.8)	
Primary therapy outcome, n (%)[a]			0.145
Partial remission	64 (14.0)	46 (10.0)	
Stable disease	70 (15.3)	76 (16.6)	
Progressive disease	28 (6.1)	36 (7.9)	
Complete remission	62 (13.5)	76 (16.6)	
Sex, n (%)[a]			0.221
Female	112 (21.2)	127 (24.1)	
Male	152 (28.8)	137 (25.9)	
Age, n (%)[a]			0.019
≤40	118 (22.3)	146 (27.7)	
>40	146 (27.7)	118 (22.3)	
Median age (IQR)[b]	42.5 (32, 54)	38 (32, 51)	0.071

[a]Fisher's exact test or χ^2 test; [b]Wilcoxon signed-rank test. IDH, isocitrate dehydrogenase; WT, wild-type; MUT, mutant; WHO, World Health Organization; SPTBN2. Spectrin β non-erythrocytic 2.

University of California, Santa Cruz (UCSC) Xena database analysis and Kaplan-Meier plotter analysis. The UCSC Xena database (http://xena.ucsc.edu/; accessed on 16 August 2022) supports the visualization and analysis of correlations between genomic and/or phenotypic variables. The database contains numerous public datasets, including data from TCGA. The database provides information on gene expression and survival outcomes. The expression and survival curve of lncRNAs was obtained by combining the GEPIA database (http://gepia.cancer-pku.cn/detail.php; accession no. GEPIA2) (19) and the 'survival' package-derived R Project (http://cran.r-project.org/package=survival) (23).

TIMER database analysis. TIMER (https://cistrome.shinyapps.io/timer/; accessed on 16 August 2022; version 2.0) is a comprehensive database established for the systematical analysis of tumor-infiltrating immune cells and their clinical impact. TIMER was also employed to analyze the relationship between SPTBN2 expression and immune infiltrates in LGG. P<0.05 was considered to indicate a statistically significant difference. The survival module assessed the association between clinical outcomes and the abundance of immune infiltrates.

Immune infiltration analysis. The level of tumor immune infiltrates was identified using a single sample GSEA (ssGSEA) method with the Gene Set Variation Analysis R package (17) based on TCGA data sets (https://tcga-data.nci.nih.gov/tcga/; V33.0; accession no. phs001145) (24). The Spearman correlation test was used to calculate the correlation analysis between *SPTBN2* and 24 immune cell types. Graphs and figures were generated using the ggplot2 R package (version 3.6.3) (https://cran.r-project.org/package=ggplot2) (23). The correlation between SPTBN2 and gene markers of immune cells was derived from GEPIA.

Enrichment analysis of Gene Set Enrichment Analysis (GSEA). The tumor samples were divided into SPTBN2-low and SPTBN2-high groups according to the data downloaded from the TCGA database (https://tcga-data.nci.nih.gov/tcga/; V33.0; accession no. phs001145) (24). The R package DESeq2 (version 1.26.0) was used to conduct the GSEA between SPTBN2-low and SPTBN2-high groups (25). Heatmap generation was performed with the R package (version 3.6.3) (22). The top 25 negative and top 25 positive correlations and these genes were selected as the top 50 correlation-ranked probes. Adjusted P-value <0.05 and false discovery rate (FDR) q-value <0.25 were considered statistically significant.

University of Alabama at Birmingham Cancer (UALCAN) data analysis portal. UALCAN is a comprehensive and interactive web resource for analyzing cancer OMICS data (26).

UALCAN was used to generate graphs and plots depicting survival information of miRNAs and lncRNAs in patients with LGG.

The Human Protein Atlas (THPA) analysis. THPA (version 21.1), a roadmap to generate renewable protein binders to the human proteome by integrating various omics technologies (including antibody-based imaging, mass spectrometry-based proteomics and transcriptomics), was used to assess *SPTBN2* expression of LGG and normal tissues. The *SPTBN2* expression of normal brain tissues and glioma tissues were detected using immunohistochemical data from THPA (27).

Tissue samples. The tissues of the patients (recruited June 2021 to January 2022) were obtained from the Department of Neurosurgery, The First Hospital of Fujian Medical University (Fuzhou, China). Glioma tissues were from first-onset cases that had not received any treatment before surgery. A total of five glioma tissues [4 World Health Organization (WHO) grade 2 glioma tissues and 1 WHO grade 3 glioma tissue] were used. The normal cerebral tissues were obtained from patients with severe traumatic brain injury undergoing internal decompression surgery. The inclusion criteria were as follows: i) The patients were >18 years of age; and ii) the patients had severe traumatic brain injury and required internal decompression surgery. The exclusion criteria were as follows: i) The patient was <18 years old; ii) the patient had other tumors in combination; iii) the patient did not provide consent; and iv) there was no serious damage or bleeding in the brain tissue taken. A total of 3 normal cerebral tissues were obtained from patients with severe traumatic brain injury undergoing internal decompression operation. The group of glioma samples comprised 5 patients (3 males and 2 females; age, 45.67±18.18 years), and the group of internal decompression samples comprised 3 patients (1 male and 2 females; age, 32.20±14.62 years). Resected samples were immediately frozen by liquid nitrogen and stored at -80˚C until use. The diagnosis of gliomas was confirmed by the pathologist through postoperative histological examination according to The 2021 WHO Classification of Tumors of the Central Nervous System (28). The pathologist was independent from the study. The diagnosis of human tumors is based on codes specified by the International Classification of Diseases (ICD) (29). The ICD was available from http://www.who.int/classifications/icd/en/. The Ethics Committee of the First Affiliated Hospital of Fujian Medical University (Fuzhou, China) approved the study protocol. All patients provided written informed consent.

Western blotting assay. Cells were lysed in NP-40 buffer (Wuhan Boster Biological Technology, Ltd.) with protease inhibitor cocktail (MedChemExpress; cat. no. HY-K0010; 1:99) and phosphatase inhibitor cocktail III (MedChemExpress; cat. no. HY-K0023; 1:99). The proteins were extracted from tissue samples using RIPA lysis buffer (Beyotime Institute of Biotechnology; cat. no. P0013B) with protease inhibitor cocktail (MedChemExpress; cat. no. HY-K0010; 1:99) and phosphatase inhibitor cocktail III (MedChemExpress; cat. no. HY-K0023; 1:99). Protein levels were determined by bicinchoninic acid assay. Equal amounts of proteins (10 μg) extracted from tissue samples and cells were separated by 12% SDS-PAGE and transferred onto a 0.45-μm PVDF membrane (Amersham; Cytiva). Membranes were blocked with 5% skimmed milk [Beijing Solarbio Science & Technology Co., Ltd.; cat. no. D8340; with 1X TBST (TBS with 0.1% Tween-20)] for 2 h at room temperature. Next, the membranes were probed with primary antibodies for β-actin (1:50,000; cat. no. AC026; ABclonal Biotech Co., Ltd.) and anti-SPTBN2 (1:1,000; cat. no. 55107-1-AP; ProteinTech Group, Inc.) overnight at 4˚C. After three washes (1X TBST), the membranes were incubated with goat anti-rabbit IgG horseradish peroxidase-conjugated secondary antibodies (1:5,000; cat. no. SA00001-2; ProteinTech Group, Inc.) for 1 h at 37˚C. After three washes (1X TBST), target proteins were detected by ECL solution (Vazyme Biotech Co., Ltd.) on Amersham Imager 680 System (Amersham; Cytiva).

Statistical analysis. *SPTBN2* expression analysis was conducted with the GEPIA, TIMER, THPA, and R projects using the 'ggplot2' package (version 3.6.3) (https://cran.r-project.org/package=ggplot2). Analysis of correlation was performed using Spearman's test. Survivals, including OS and DFS, were performed with GEPIA, ENCORI, TIMER and R projects (version 3.6.3) (23). The association between SPTBN2 expression and clinicopathologic features was evaluated using Fisher's exact test, χ^2 test, Wilcoxon signed-rank test and logistic regression. In addition, the Kaplan-Meier method and Cox regression were used to evaluate the role of *SPTBN2* expression in prognosis. $P<0.05$ was considered to indicate a statistically significant difference.

Results

Expression and survival analysis for SPTBN2 in pan-cancer studies. To explore the potential roles of *SPTBN2* in carcinogenesis, the expression of *SPTBN2* in various types of human cancer and corresponding TCGA and GTEx normal tissues were analyzed. Differences in *SPTBN2* were detected in 27 types of cancer, except cholangiocarcinoma (CHOL), kidney chromosome cancer (KICH), mesothelioma (MESO), pheochromocytoma and paraganglioma (PCPG), sarcomas (SARC) and uveal melanoma (UVM) (Fig. 1A). SPTBN2 expression was downregulated In LGG samples compared with corresponding TCGA and GTEx normal tissues (Fig. 1). For OS, higher expression of *SPTBN2* had an unfavorable prognosis in kidney renal clear cell carcinoma (KIRC), ovarian serous cystadenocarcinoma (OV), prostate adenocarcinoma (PAAD) and UVM (Fig. 1B-F). Moreover, higher expression of SPTBN2 was significantly associated with short DFS in KIRC and PAAD (Fig. 1G-K). However, lower expression of *SPTBN2* was associated with short OS and DFS in LGG. Higher expression of SPTBN2 was associated with poor prognosis in KIRC and PAAD (Fig. 1B, E, G and J), while lower expression of *SPTBN2* was associated with an unfavorable outcome in LGG (Fig. 1C and H).

Low SPTBN2 expression is associated with poor clinicopathological features of LGG. As shown in Table I, 528 LGG cases were collected from TCGA datasets with complete clinical and gene expression data. Patients with LGG were

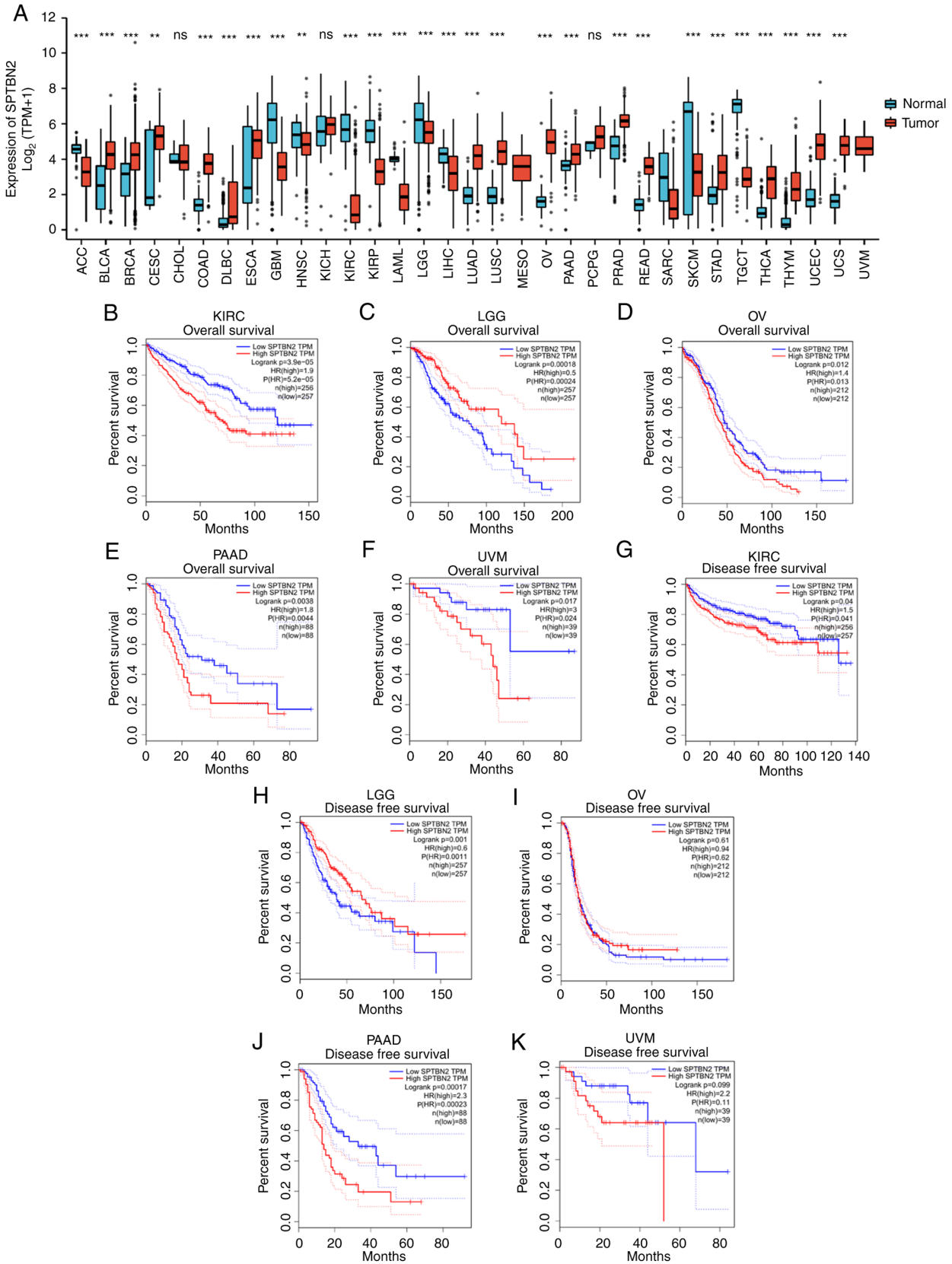

Figure 1. Expression and survival analysis for SPTBN2 in pan-cancer types. (A) The expression of SPTBN2 in pan-cancer types of human cancer compared with corresponding TCGA and GTEx normal tissues was performed. Significant differences in SPTBN2 were detected in 27 types of cancer, except CHOL, KICH, MESO, PCPG, SARC and UVM. SPTBN2 was downregulated in LGG. (B) For OS, higher expression of SPTBN2 had an unfavorable prognosis in KIRC. (C) Lower expression of SPTBN2 correlated with short OS in LGG. Higher expression of SPTBN2 had an unfavorable prognosis in (D) OV, (E) PAAD and (F) UVM. (G) For DFS, higher expression of SPTBN2 correlated with short DFS in KIRC. (H) Lower expression of SPTBN2 correlated with DFS in LGG. (I) Lower expression of SPTBN2 was not associated with DFS in OV. (J) Higher expression of SPTBN2 correlated with short DFS in PAAD. (K) Higher expression of SPTBN2 was not associated with DFS in UVM. **P<0.01 and ***P<0.001. CHOL, cholangiocarcinoma; KICH, kidney chromosome cancer; MESO, mesothelioma; PCPG, pheochromocytoma and paraganglioma; SARC, sarcomas; UCM, uveal melanoma; KIRC, kidney renal clear cell carcinoma; OV, ovarian serous cystadenocarcinoma; PAAD, prostate adenocarcinoma.

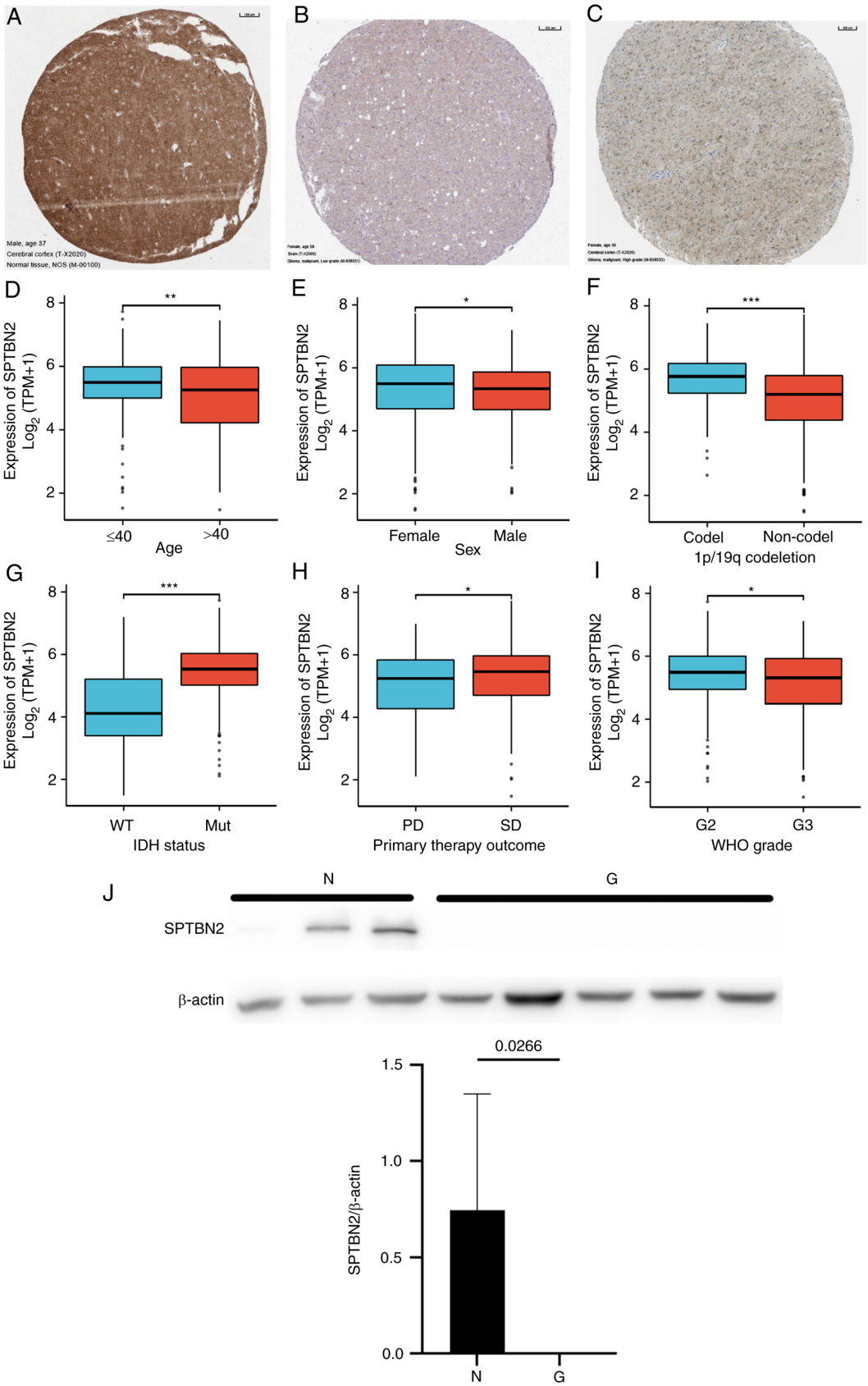

Figure 2. Correlation of SPTBN2 mRNA and clinical status. (A-C) Immunohistochemical analysis of SPTBN2 was conducted on normal brain and glioma tissues using The Human Protein Atlas database. (A) Abundant expression of SPTBN2 was found in the normal cerebral cortex. (B) No expression and (C) weak expression were detected in low-grade glioma. The mRNA of SPTBN2 in LGG from TCGA was analyzed using the TCGA colonic adenocarcinoma and rectal adenocarcinoma data sets according to (D) age, (E) sex, (F) 1p/19q codeletion, (G) IDH status, (H) primary therapy outcome (I) and WHO grade. Low SPTBN2 expression was significantly correlated with older age, males, 1p/19q non-codeletion, wild-type IDH status, PD and WHO grade. (J) Western blotting assay results showed that the amount of SPTBN2 in LGG was significantly lower compared with that in normal brain tissues (P=0.0266). *P<0.05, **P<0.01, ***P<0.001. Ns, no significant difference; SPTBN2, spectrin β non-erythrocytic 2; TCGA, The Cancer Genome Atlas; LGG, low-grade gliomas; IDH, isocitrate dehydrogenase; PD, progressive disease; WHO, World Health Organization; WT, wild-type; Mut, mutation; SD, stable disease.

Table II. Multivariate logistic regression analysis of how SPTBN2 is associated with clinicopathological parameters in LGG.

Characteristics	Total (n)	Odds ratio (OR)	P-value[a]
WHO grade (G3 vs. G2)	467	0.776 (0.539-1.117)	0.173
1p/19q codeletion (non-codel vs. codel)	528	0.323 (0.219-0.473)	<0.001
Primary therapy outcome (PR + CR vs. PD + SD)	458	1.367 (0.945-1.982)	0.098
Sex (male vs. female)	528	0.795 (0.563-1.120)	0.190
Age (>40 vs. ≤40)	528	0.653 (0.463-0.920)	0.015
IDH status (Mut vs. WT)	525	4.664 (2.822-8.014)	<0.001

[a]Multivariate logistic regression; IDH, isocitrate dehydrogenase; WT, wild-type; MUT, mutant; PR, progressive disease; CR, complete remission; PD, partial remission; SD, stable disease.

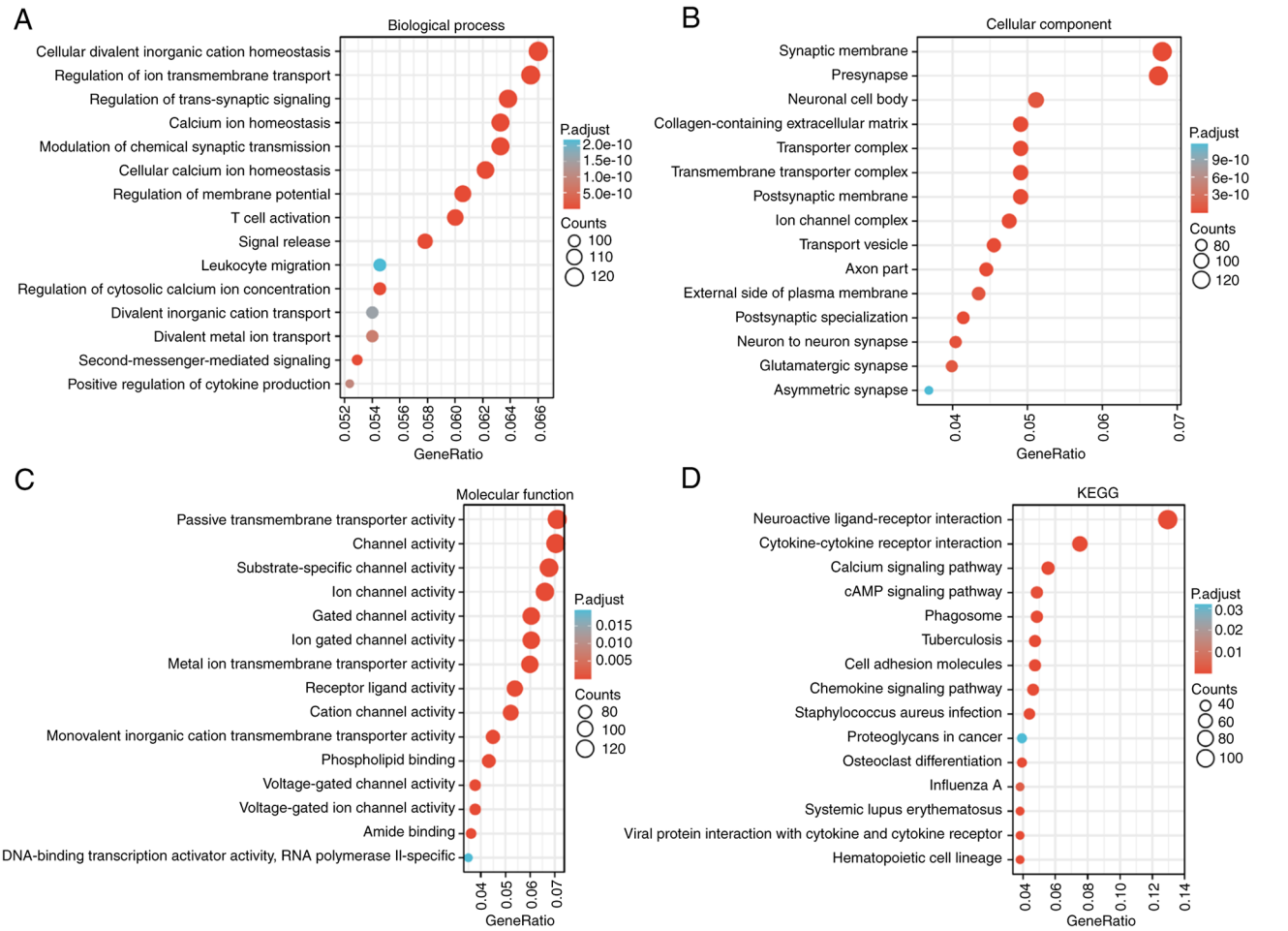

Figure 3. Enrichment analysis of SPTBN2 functional networks in LGG. Gene Ontology enrichment of (A) biological process, (B) cellular components and (C) molecular function for genes related to SPTBN2. (D) KEGG pathway map of signaling pathway associated with SPTBN2 expression. SPTBN2, spectrin β non-erythrocytic 2; LGG, low-grade gliomas.

categorized into *SPTBN2*-high (n=264) and *SPTBN2*-low (n=264) groups. The association between SPTBN2 expression and clinicopathological characteristics of patients with LGG was evaluated (Table I and Fig. 2). Immunohistochemical analysis of *SPTBN2* was conducted on normal brain and glioma tissues using the THPA database (Fig. 2A-C). A significant correlation between low *SPTBN2* mRNA expression and poor clinicopathological features was detected, including elders (P=0.019; Fig. 2D), males (P<0.05; Fig. 2E), 1p/19q non-codeletion (P<0.001; Fig. 2F), wild-type isocitrate dehydrogenase (IDH) status (P<0.001; Fig. 2G), primary therapy (P<0.05; Fig. 2H) and WHO grade (P<0.05; Fig. 2I). The western blotting assay results demonstrated that the expression of *SPTBN2* in LGG was significantly lower compared with that in normal brain tissues (P=0.0266; Fig. 2J). Furthermore, univariate logistic regression analysis (Table II) indicated that *SPTBN2* mRNA expression was closely associated with 1p/19q codeletion [OR=0.323; 95% confidence interval

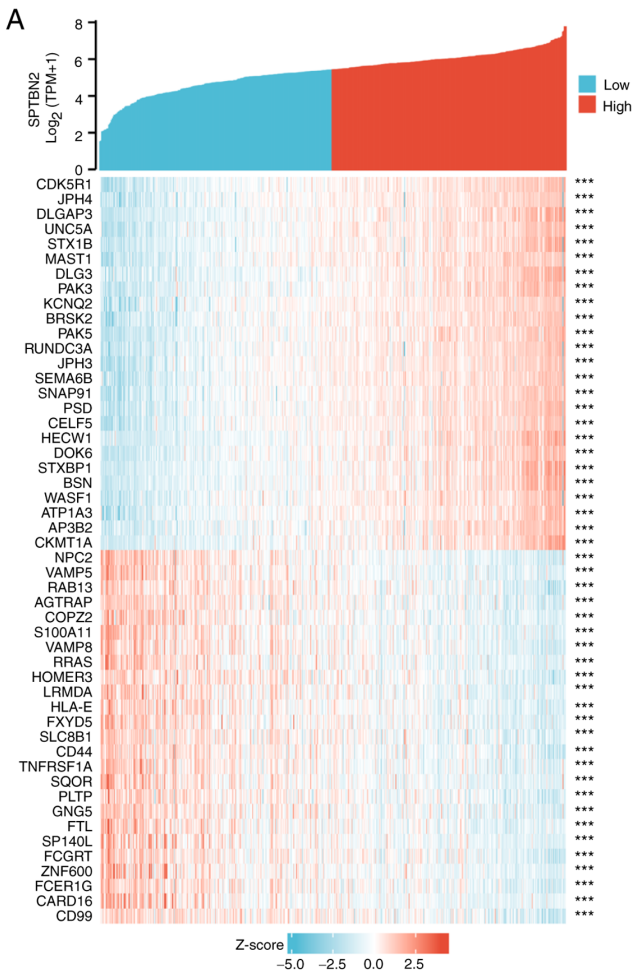

B

miRNA	geneName	R-value	P-value
hsa-miR-214-3p	SPTBN2	−0.086	4.80×10^{-2}
hsa-miR-15a-5p	SPTBN2	−0.227	1.42×10^{-7}
hsa-miR-16-5p	SPTBN2	−0.133	2.19×10^{-3}
hsa-miR-15b-5p	SPTBN2	−0.215	7.01×10^{-7}
hsa-miR-34c-5p	SPTBN2	−0.155	3.58×10^{-4}
hsa-miR-424-5p	SPTBN2	−0.191	1.01×10^{-5}

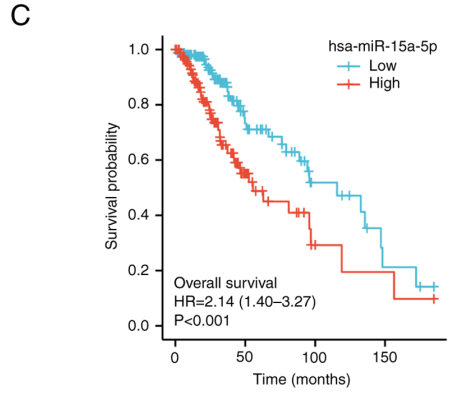

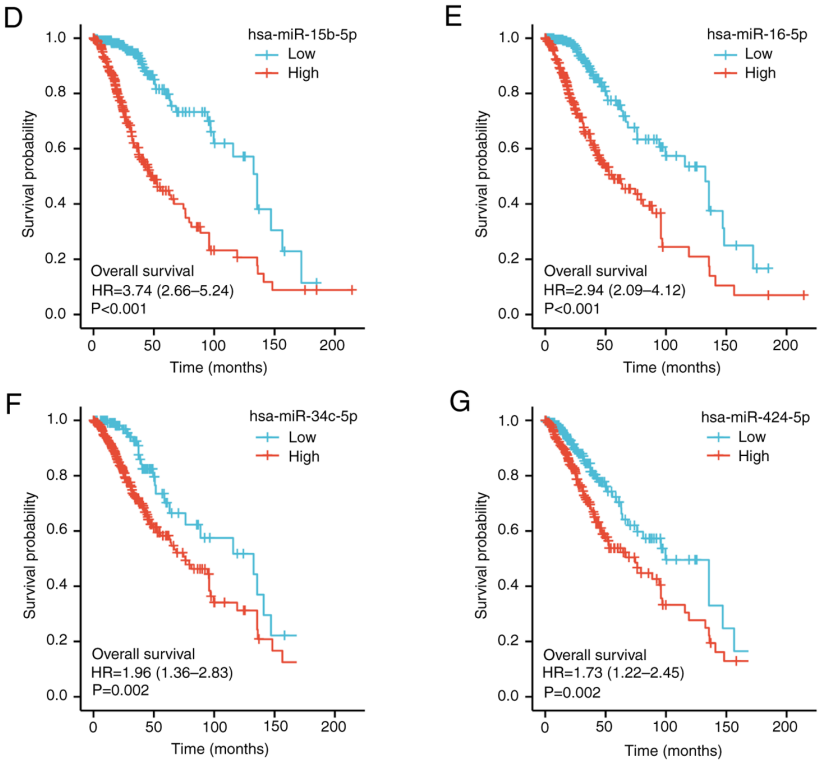

Figure 4. Analysis of candidate miRNAs and lncRNAs binding to SPTBN2. (A) Heatmap showing the top 50 genes in LGG that were positively and negatively associated with SPTBN2. Red represents positively related genes, and blue represents negatively related genes. (B) All six candidate miRNAs, including hsa-miR-214-3p, hsa-miR-15a-5p, hsa-miR-16-5p, hsa-miR-15b-5p, hsa-miR-34c-5p, and hsa-miR-424-5p, that are negatively correlated with SPTBN2 mRNA expression. (C-G) The R package assessed the overall survival analysis of 6 candidate miRNAs. Higher expression of (C) hsa-miR-15a-5p, (D) hsa-miR-15b-5p, (E) hsa-miR-16-5p, (F) hsa-miR-34c-5p and (G) hsa-miR-424-5p was associated with poor prognosis. LGG, low-grade glioma; SPTBN2, Spectrin β non-erythrocytic 2; miR, microRNA.

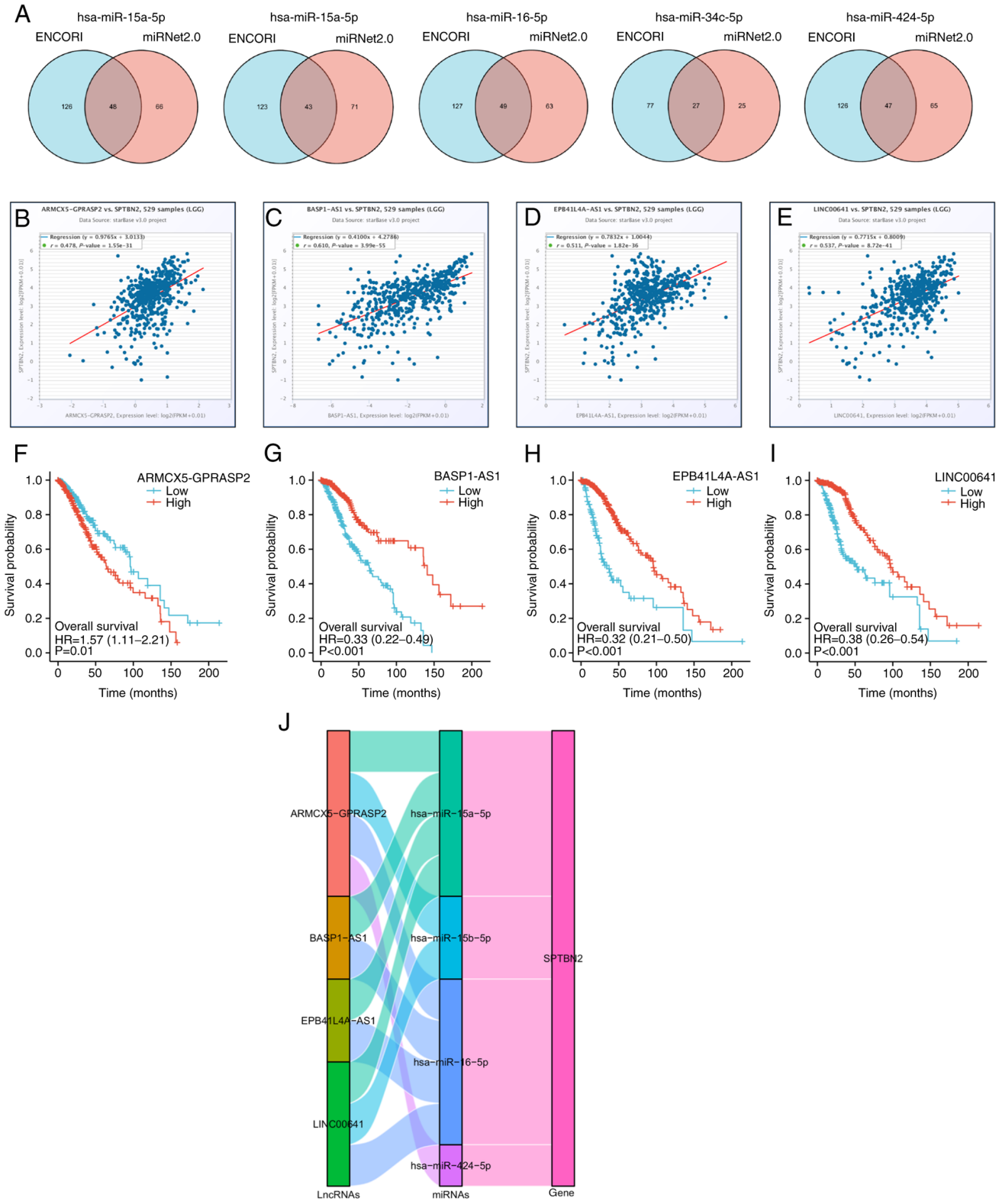

Figure 5. Correlation of predictive lncRNAs and SPTBN2, survival analysis of predictive lncRNAs and Sankey diagram of the lncRNA-miRNA-mRNA SPTBN2 regulatory network. (A) Venn graph of predictive miRNA-targeted lncRNAs in ENCORI and miRNet2.0. LncRNAs (B) ARMCX5-GPRASP2, (C) BASP1-AS1, (D) EPB41L4A-AS1 (E) and LINC00641 were positively correlated with SPTBN2 mRNA expression. Moreover, low expression of (F) ARMCX5-GPRASP2 and high expression of (G) BASP-AS1, (H) EPB41L4A-AS1 and (I) LINC00641 were associated with a favorable outcome of LGG. (J) Sankey diagram shows the lncRNA-miRNA-mRNA SPTBN2 regulatory network in line with the ceRNA hypothesis. lncRNA, long non-coding RNA; SPTBN2, Spectrin β non-erythrocytic 2; miR, microRNA.

(CI), 0.219-0.473; P<0.001], IDH status (OR=4.664; 95% CI, 2.822-8.014; P<0.001) and older ages (OR=0.653; 95% CI, 0.463-0.920; P=0.015).

Predicted biological function and pathways of SPTBN2 in LGG. GSEA analysis was performed to identify the possible biological pathways regulated by *SPTBN2* between

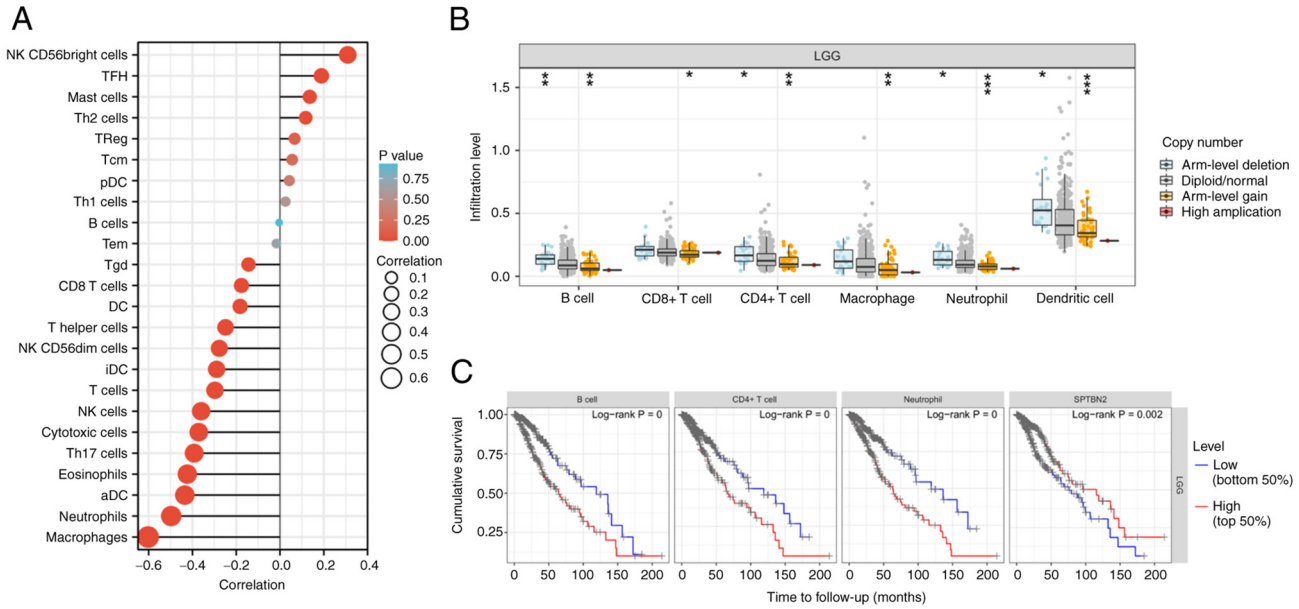

Figure 6. Relationship of immune cell infiltration and survival with SPTBN2 level in LGG. (A) Association between SPTBN2 expression and 24 tumor-infiltrating lymphocytes. (B) A significant change in immune cell infiltration levels under various copy numbers of SPTBN2 in LGG, including B cells, $CD8^+$ T cells, $CD4^+$ T cells, macrophage, neutrophils and dendritic cells were observed. (C) Survival module explored the association between clinical outcome and abundance of immune infiltrates and SPTBN2 expression. Higher immune cell infiltration (B cells, $CD4^+$ cells and neutrophils) and low expression of SPTBN2 were significantly positively associated with poor outcomes. *P<0.05, **P<0.01 and ***P<0.001. LGG, low-grade glioma; SPTBN2, Spectrin β non-erythrocytic 2.

SPTBN2-high and *SPTBN2*-low groups. As shown in Fig. 3A-D, several signal KEGG pathways were significantly associated with *SPTBN2* expression, including 'neuroactive ligand-receptor interaction', 'cytokine-cytokine receptor interaction', 'calcium signaling pathway' and 'cAMP signaling pathway'. A heatmap showed the top 50 genes in LGGs that were positively and negatively associated with *SPTBN2* (Fig. 4A). The red color denoted positively correlated genes, and the blue color denoted negatively correlated (Fig. 4A). Briefly, SPTBN2 was positively associated with *CDK5R1, PAK5, UNC5A, DLGAP3* and *CELF5*. By contrast, *SPTBN2* was negatively associated with *CD99, HOMER3, PTLP, SLC8B1 and CD44*.

Analysis of candidate miRNAs and lncRNAs that bind to SPTBN2. According to the ceRNA hypothesis (30), miRNAs negatively correlate with SPTBN2, while lncRNAs correlate positively with *SPTBN2*. Candidate miRNAs must negatively correlate with SPTBN2 expression and be statistically associated with prognosis in LGG (30). Subsequently, candidate lncRNAs that might bind to the candidate miRNAs were generated using ENCORI. The enrolled lncRNAs must positively correlate with the expression of *SPTBN2* and the prognosis of low-grade gliomas. MiRNAs and lncRNAs were rigorously screened out based on the ceRNA hypothesis.

Predicted miRNAs that could competitively bind to *SPTBN2* were investigated. A total of six candidate miRNAs, including *hsa-miR-214-3p, hsa-miR-15a-5p, hsa-miR-16-5p, hsa-miR-15b-5p, hsa-miR-34c-5p* and *hsa-miR-424-5*p, were revealed (Fig. 4B). Higher expression of five miRNAs, *hsa-miR-15a-5p* (Fig. 4C), *hsa-miR-15b-5p* (Fig. 4D), *hsa-miR-16-5p* (Fig. 4E), *hsa-miR-34c-5p* (Fig. 4F) and hsa-miR-424-5p (Fig. 4G) were associated with poor prognosis in LGG. Subsequently, 48 candidate lncRNAs associated with *hsa-miR-15a-5p* were regulated in LGG (Fig. 5A), of which 22 candidate lncRNAs related to *hsa-miR-15a-5p* were downregulated in LGG. The statistical significances of four lncRNAs (*BASP1-AS1, EPB41L4A-AS1, LINC00641 and ARMCX5-GPRASP2*) for predicting the prognosis of LGG were obtained, while the statistical significance of the other 18 LncRNAs were not. In addition, a positive correlation of candidate lncRNAs and SPTBN2 was revealed by ENCORI (Fig. 5B-E). A total of 43 candidate lncRNAs associated with *hsa-miR-15b-5p* were regulated in LGG (Fig. 5A), of which 21 candidate lncRNAs related to *hsa-miR-15b-5p* were downregulated in LGG. The statistical significances of two lncRNAs (*LINC00641* and *ARMCX5-GPRASP2*) for predicting the prognosis of LGG were detected, while the statistical significance of the other 19 lncRNAs were not. A total of 49 lncRNAs that were associated with *hsa-miR-16-5p* underwent regulation in LGG (Fig. 5A), with 22 of these lncRNAs experiencing downregulation. The statistical significances of *ARMCX5-GPRASP2* (Fig. 5F), *BASP1-AS1* (Fig. 5G), *EPB41L4A-AS1* (Fig. 5H), *LINC00641* (Fig. 5I) were investigated to predict the prognosis of LGG, while the statistical significance of the other 18 lncRNAs were not. In LGG, a total of 27 candidate lncRNAs that were linked to *hsa-miR-34c-5p* exhibited regulation, as demonstrated in Fig. 5A. Among these, 15 candidate lncRNAs that were associated with *hsa-miR-34c-5p* were observed to be downregulated. A significant correlation was not found between all lncRNAs and prognosis for LGG. A total of 22 candidate lncRNAs associated with *hsa-miR-424-5p* were downregulated in LGG. A total of 47 candidate lncRNAs associated with *hsa-miR-424-5p* were downregulated in LGG (Fig. 5A), of which 22 candidate

Table III. Correlation analysis between SPTBN2 and biomarkers of immune cells in LGG.

Immune cells	Biomarker	R value	P-value
T cell (general)	CD3D	-0.26	$3.5x10^{-9}$
	CD3E	-0.26	$2.6x10^{-9}$
	CD2	-0.26	$2.7x10^{-9}$
$CD8^+$ T cell	CD8A	-0.07	$1.0x10^{-1}$
	CD8B	-0.24	$2.9x10^{-8}$
Tumor-associated macrophages	CCL2	-0.18	$4.0x10^{-5}$
	CD68	-0.41	$2.1x10^{-22}$
B Cell	CD19	-0.13	$3.8x10^{-3}$
	CD79A	-0.1	$1.8x10^{-2}$
Macrophage/M1	NOS2	-0.03	$5.6x10^{-1}$
	IRF5	-0.43	$2.6x10^{-25}$
	PTGS2	0.08	$7.1x10^{-2}$
Macrophage/M2	CD163	-0.25	$7.6x10^{-9}$
	VSIG4	-0.34	$4.3x10^{-15}$
	MS4A4A	-0.31	$3.3x10^{-13}$
Neutrophil	CEACAM8	-0.07	$1.4x10^{-1}$
	ITGAM	-0.4	$2.0x10^{-21}$
	CCR7	-0.15	$7.3x10^{-4}$
Natural killer cell	KIR2DL1	-0.09	$4.0x10^{-2}$
	KIR2DL3	-0.11	$8.9x10^{-3}$
	KIR2DL4	-0.22	$6.7x10^{-7}$
	KIR3DL1	-0.15	$6.8x10^{-4}$
	KIR3DL2	-0.16	$3.3x10^{-4}$
	KIR3DL2	-0.16	$3.3x10^{-4}$
	KIR2DS4	-0.09	$4.5x10^{-2}$
Dendritic cells	HLA-DPB1	-0.35	$9.1x10^{-17}$
	HLA-DQB1	-0.28	$8.6x10^{-11}$
	HLA-DRA	-0.36	$3.6x10^{-17}$
	HLA-DPA1	-0.32	$3.6x10^{-14}$
	CD11c/ITGAX	-0.36	$2.0x10^{-17}$

Correlation analyses performed using Spearman's rank correlation test. NOS2, nitric oxide synthase 2; IRF5, interferon regulatory factor 5; PTGS2, prostaglandin-endoperoxide synthase 2; VSIG4, V-set and immunoglobulin domain containing 4; CEACAM8, carcinoembryonic antigen-related cell adhesion molecule 8; ITGAM, integrin subunit α M; CCR7, C-C chemokine receptor type 7; KIR, killer cell immunoglobulin-like receptor.

lncRNAs associated with *hsa-miR-424-5p* were downregulated. Finally, the statistical significance of four lncRNAs, including *ARMCX5-GPRASP2, BASP1-AS1, EPB41L4A-AS1 and LINC00641*, were detected to predict predict the prognosis of high and low expression levels in LGG (Fig. 5F-I).. In LGG patients, high expression of ARMCX5-GPRASP2 was associated with shorter survival time, while low expression of BASP1-AS1, EPB41L4A-AS1 and LINC00641 was associated with shorter survival time.

The Sankey diagram presents the *lncRNA-miRNA-SPTBN2* regulatory network according to the ceRNA hypothesis (Fig. 5J). Overall, four lncRNAs (*ARMCX5-GPRASP2*, *BASP1-AS1*, *EPB41L4A-AS1* and *LINC00641*) were involved in the regulation of *SPTBN2* via five miRNAs (*hsa-miR-15a-5p*, *hsa-miR-15b-5p*, *hsa-miR-16-5p* and *hsa-miR-424-5p*) in LGG.

Association of immune cell infiltration, overall survival, immune checkpoints and SPTBN2 level in LGG. Infiltration of immune cells, including 'macrophages', 'neutrophils', 'dendritic cells', 'NK cells' and 'T cells', were negatively correlated with *SPTBN2* expression (Fig. 6A). In addition, significant changes in immune cell infiltration with various copy numbers of *SPTBN2* in LGG, including B cells, $CD8^+$ T cells, $CD4^+$ T cells, macrophage, neutrophils, and dendritic cells were observed (Fig. 6B). Correlation analysis between *SPTBN2* and biomarkers of immune cells in LGG are presented in Table III. The survival module explored the association between clinical outcomes and the abundance of *SPTBN2*-related immune infiltrates (Fig. 6C). Higher immune infiltrates (B cells, $CD4^+$ cells, neutrophils) and low expression of *SPTBN2* were significantly positively associated with poor outcomes (Fig. 6C). Moreover, *SPTBN2* mRNA expression was negatively correlated with

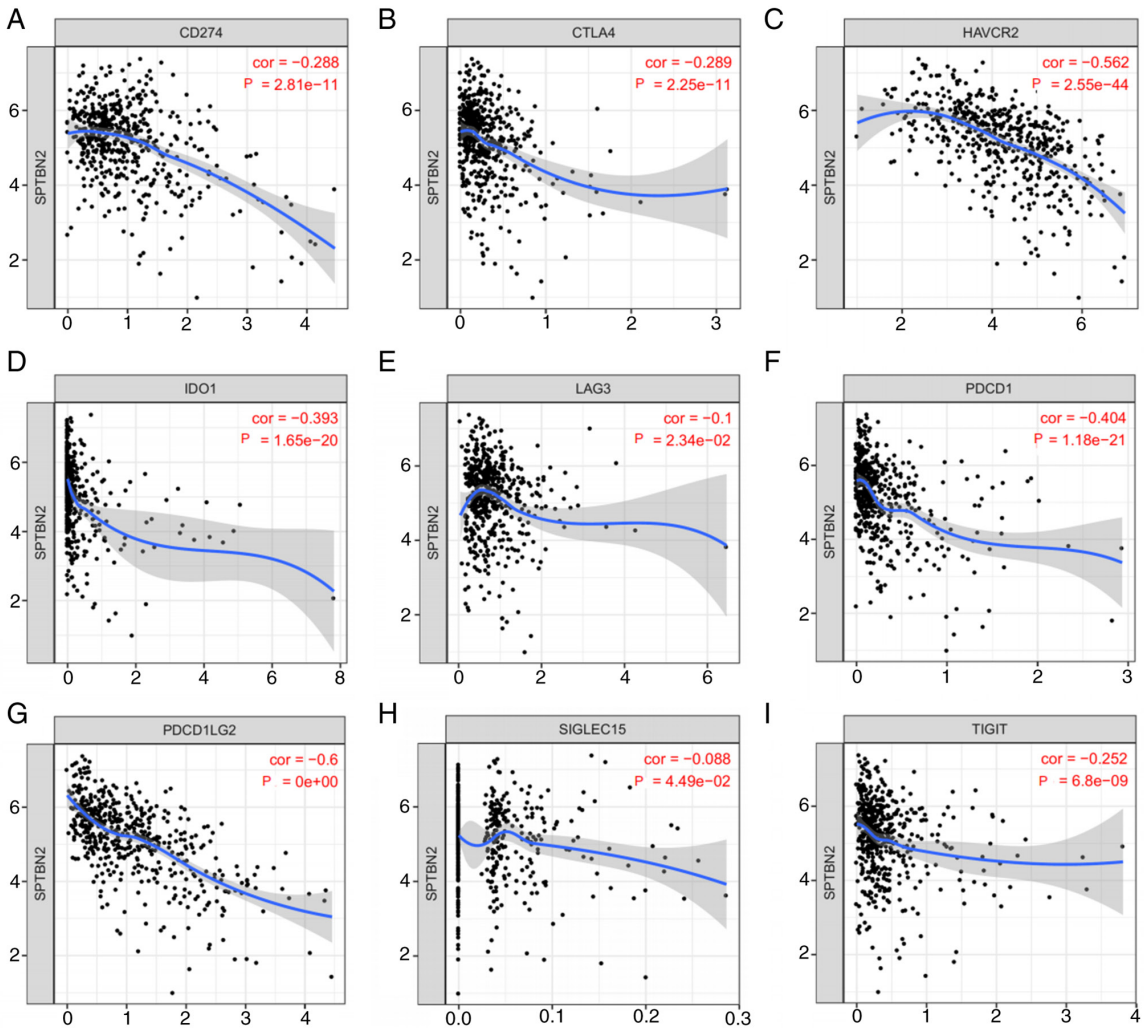

Figure 7. Relationship between SPTBN2 and immune checkpoints in LGG. SPTBN2 expression and immune checkpoints in LGG were assessed. *SPTBN2* mRNA expression was significantly negatively correlated with (A) *CD274*, (B) *CTLA4*, (C) *HAVCR2*, (D) *IDO1*, (E) *LAG3*, (F) *PDCD1*, (G) *PDCD1LG2*, (H) *SIGLEC15* and (I) *TIGIT*. *CD274*, cluster of differentiation 274; *PDCD1*, programmed cell death 1; *CTLA4*, cytotoxic T lymphocyte antigen 4; *SIGLEC15*, sialic acid-binding immunoglobulin-like lectin 15; *TIGIT*, T cell immunoreceptor with Ig and immunoreceptor tyrosine-based inhibitory domains; *HAVCR2*, hepatitis A virus cellular receptor 2; *LAG3*, lymphocyte activation gene-3; *IDO1*, indoleamine 2,3-dioxygenase 1; *PDCD1LG2*, programmed cell death 1 ligand 2.

nine immune checkpoints: *CD274, CTLA4, HAVCR2, IDO1, LAG3, PDCD1, PDCD1LG2, SIGLEC15 and TIGIT* (Fig. 7).

Discussion

Management of patients with low-grade gliomas is mainly based on clinical prognostic factors. Median survival varies from 3.2 (high-risk LGG) to 7.8 years (low-risk LGG) (31). Despite improved advances in diagnosis and therapeutic techniques, the majority of LGGs progress clinically to GBM over time (7). Moreover, high-risk LGGs resemble GBM and correlate with poor outcomes (32). Evidence suggests that *SPTBN2* plays important roles in tumor initiation and progression in multiple types of human cancer, including ovarian cancer, endometrioid endometrial cancer and lung cancer adenocarcinoma (13,15). However, the expression, function, and molecular mechanism of *SPTBN2* in LGG remain unclear.

The present study conducted a pan-cancer analysis of the expression of SPTBN2 using TCGA and GTEx data. Previous studies have indicated that *SPTBN2* is highly expressed in lung adenocarcinoma and endometrioid endometrial cancer, is positively correlated with unfavorable prognosis and promotes cancer proliferation, invasion, and migration of cells (13,15). In the present study, the TCGA and GTEx databases analysis revealed a statistically significant decrease in *SPTBN2* expression in LGG samples compared with normal tissues. *SPTBN2* has been previously reported in the development of neurological disorders and cancer (13,15). The low expression of *SPTBN2* may be associated with the expression of tumor suppressors in LGG (16). Additionally, *SPTBN2* has recently been identified as a key gene in the development of seven different types of cancer, and it has been identified as a marker for the recognition of cancer patterns (33). However, survival analysis indicated that patients with LGG with low expression *SPTBN2* had a worse prognosis. An age >40 years has been reported to be associated with an inferior prognosis (34). Known favorable molecular prognostic factors of LGG contain codeletion of chromosome 1p/19q and isocitrate dehydrogenase mutation (31). IDH wild-type LGGs mimicking high-grade

gliomas are associated with poor outcomes (32). The present study revealed that low expression of *SPTBN2* was significantly correlated with older adults (>40 years), 1p/19q non-codeletion and wild-type IDH status, which were associated with an unfavorable outcome.

It is well known that ncRNAs, including miRNAs and lncRNAs, play key roles in regulating gene expression via the ceRNA mechanism (14,15,35). The present study used seven prediction programs to identify the candidate miRNAs of *SPTBN2*. Lastly, six miRNAs were obtained, including *hsa-miR-214-3p, hsa-miR-15a-5p, hsa-miR-16-5p, hsa-miR-15b-5p, hsa-miR-34c-5p, and hsa-miR-424-5p*. In addition, 5 miRNAs, including *hsa-miR-15a-5p, hsa-miR-16-5p, hsa-miR-15b-5p, hsa-miR-34c-5p and hsa-miR-424-5p*, had pro-tumorigenic effects and were correlated with poor prognosis in LGG. Higher expression of *hsa-miR-15b-5p* has been reported to be associated with a short survival time of patients with LGG (36). Has-miR-15a-5p promotes the proliferation and invasion of colorectal cancer by targeting CCND1 (37). Hsa-mir-16-5p is downregulated in giant cell tumors (38). Ectopic expression of hsa-miR-424-5p leads to enhanced growth of gastric cancer cells by targeting LATS1 (39). The present study revealed that higher expression levels of *hsa-miR-15a-5p, hsa-miR-16-5p, hsa-miR-34c-5p* and *hsa-miR-424-5p*, were correlated with lower *SPTBN2* mRNA expression and unfavorable prognosis in LGG. *SPTBN2* was associated with poor prognosis and regulated by miRNA-1827 in ovarian cancer (16). *SPTBN2* was also a target of *miR-424-5p* and promoted endometrial cancer metastasis via the PI3K/AKT pathway (15).

Based on the ceRNA hypothesis, the potential lncRNAs were positively related to *SPTBN2* in LGG (30). A comprehensive, integrated analysis of lncRNAs indicated that the four most promising lncRNAs, including *ARMCX5-GPRASP2, BASP1-AS1, EPB41L4A-AS1 and LINC00641*, were associated with *SPTBN2* mRNA expression and prognosis of LGG. Higher expression levels of *BASP-AS1, EPB41L4A-AS1 and LINC00641* were associated with a favorable outcome of LGG, while higher expression of *ARMCX5-GPRASP2* correlated with poor prognosis in LGG. *BASP1-AS1* is a protective lncRNA and significantly impacts the proliferation of glioma cells (40). Functionally, the ectopic expression of *BASP1-AS1* promotes cell proliferation and invasion in melanoma (41). *LINC00641* is differentially expressed in various tumors and is associated with a poor prognosis (42). Decreased *LINC00641* leads to changes in tumor proliferation (42). Yang *et al* revealed that reduced expression of *LINC00641* is observed in glioma, and overexpression of *LINC00641* promotes apoptosis of glioma (43).

Nevertheless, the role of *ARMCX5-GPRASP2* and *EPB41L4A-AS1* in predicting prognosis in LGG remains unclear. Low expression of *EPB41L4A-AS1* has been detected in multiple types of human cancer and is associated with poor prognosis (44). *EPB41L4A-AS1* functions as a repressor of the Warburg effect and plays a notable role in the metabolic reprogramming of cancer (44). *EPB41L4A-AS1* also functions as an oncogene by regulating the Rho/ROCK pathway in colon cancer (45). The deletion of *ARMCX5-GPRASP2* has been associated with the novel Xq22.1 deletion syndrome in a male patient with multiple congenital abnormalities (46). The present study revealed that higher expression of *ARMCX5-GPRASP2* correlated with poor prognosis in LGG.

Previous studies have indicated that *LINC01605* can regulate m6A modification of SPTBN2 mRNA in colorectal cancer (27). In a lncRNA-miRNA-mRNA network of bladder cancer, *SPTBN2* and *hsa-miR-590-3p* affect the prognosis of patients with bladder cancer (14). Collectively, according to the ceRNA hypothesis, the Sankey plot can demonstrate the pathways by which low *SPTBN2* expression is associated with poor prognosis in LGG. The Sankey plot illustrates the *lncRNA-miRNA-SPTBN2* regulatory network based on the ceRNA hypothesis. In LGG, four lncRNAs (*ARMCX5-GPRASP2, BASP1-AS1, EPB41L4A-AS1 and LINC00641*) were regulated through five miRNAs (*hsa-miR-15a-5p, hsa-miR-15b-5p, hsa-miR-16-5p, hsa-miR-34c -5p* and *hsa-miR-424-5p*) were involved in the regulation of SPTBN2. Candidate miRNAs, lncRNAs, and SPTBN2 expression were observed to correlate with poor LGG prognosis.

Tumor cells frequently interact with the microenvironment and a variety of immune cells. Moreover, the tumor microenvironment has been shown to affect response to immune checkpoint blockade (47). An immune checkpoint blockade takes advantage of tumor immune infiltration to launch an effective immune response (47). The present study suggested that significant changes in immune infiltration with various copy numbers of SPTBN2, including B cells, $CD8^+$ T cells, $CD4^+$ T cells, macrophages, neutrophils and dendritic cells, were observed in LGG. Furthermore, higher immune cell infiltration (B cells, $CD8^+$ cells, $CD4^+$ cells, macrophages, neutrophils and dendritic cells) and low expression of SPTBN2 were significantly positively associated with poor outcomes. A previous study revealed that SPTBN2 generates adverse effects on the reduced infiltration of $CD4^+$ T cells and leads to an unsatisfactory outcome in ovarian cancer (16). The present study also assessed the relationship between SPTBN2 and immune checkpoints. The results demonstrated that SPTBN2 mRNA expression was significantly negatively correlated with nine immune checkpoints, indicating that targeting SPTBN2 might increase the efficacy of immunotherapy in LGG. However, future experiments are required to ascertain the correlation between *SPTBN2* and tumor immunity in LGG.

In summary, we elucidated that *SPTBN2* was lowly expressed and correlated with an unfavorable prognosis in LGG. We identified 6miRNAs and four lncRNAs being able to modulate *SPTBN2* in an lncRNA-miRNA-mRNA network of LGG. Furthermore, our current findings also indicated that *SPTBN2* possessed anti-tumor roles via regulating tumor immune infiltration and immune checkpoint expression. However, these results should be validated by more basic experiments and clinical trials in the future.

Acknowledgements

Not applicable.

Funding

The study was supported by the Excellent Talent Project of the First Affiliated Hospital of Fujian Medical University (grant

no. YYXQN-YPS2021), Fujian Clinical Research Center for Neurological Disease (grant no. SSJ-YJZX-1) and Fujian Key Laboratory of Precision Medicine for Cancer (grant no. ZLZDSYS-2020).

Availability of data and materials

The datasets analyzed in this study are available in the following open access repositories. TGGA: The Cancer Genome Atlas (TCGA) database (https://tcga-data.nci.nih.gov/tcga/; version V33.0; release date, May 3, 2022; dbGaP Study accession no. phs001145), GEPIA (http://gepia.cancer-pku.cn/detail.php; accessed on 16 August 2022; accession no. GEPIA2), ENCORI (http://starbase.sysu.edu.cn; accessed on 16 August 2022), miRNet2.0 (www.mirnet.ca/miRNet/home.xhtml; accessed on 16 August 2022), The UCSC Xena database (http://xena.ucsc.edu/; accessed on 16 August 2022) and TIMER (https://cistrome.shinyapps.io/timer/; accessed on 16 August 2022). The datasets used and/or analyzed during the current study are available from the corresponding author on reasonable request.

Authors' contributions

GRC**,** YBZ, SFZ, DZK and PSY designed the study. YBZ, GRC, PL and HCSG performed all bioinformatic analyses. GRC, YBZ and YWX completed the experiments. GRC, YXL, and PSY confirm the authenticity of all the raw data. YXL and DZK acquired the data, and analyzed and interpreted the data. GRC, YBZ, SFZ, and PSY drafted the manuscript. YBZ, YWX, PL and HCSG prepared the figures and interpreted the results. PSY and DZK were identified as the guarantors of the paper, taking responsibility for the integrity of the work as a whole. All authors read and approved the final manuscript.

Ethics approval and consent to participate

The present study was approved by the Ethics Committee of the First Affiliated Hospital of Fujian Medical University [approval no. MRCTA, ECFAH of FMU(2022)509]. Written informed consents were obtained from all enrolled individuals prior to their participation.

Patient consent for publication

Not applicable.

Competing interests

The authors declare that they have no competing interests.

References

1. Hua D, Tang L, Wang W, Tang S, Yu L, Zhou X, Wang Q, Sun C, Shi C, Luo W, *et al*: Improved antiglioblastoma activity and BBB permeability by conjugation of paclitaxel to a cell-penetrative MMP-2-cleavable peptide. Adv Sci (Weinh) 8: 2001960, 2021.
2. Lapointe S, Perry A and Butowski NA: Primary brain tumours in adults. Lancet 392: 432-446, 2018.
3. Lin W, Huang Z, Xu Y, Chen X, Chen T, Ye Y, Ding J, Chen Z, Chen L, Qiu X and Qiu S: A three-lncRNA signature predicts clinical outcomes in low-grade glioma patients after radiotherapy. Aging 12: 9188-9204, 2020.
4. Bhanja D, Ba D, Tuohy K, Wilding H, Trifoi M, Padmanaban V, Liu G, Sughrue M, Zacharia B, Leslie D and Mansouri A: Association of low-grade glioma diagnosis and management approach with mental health disorders: A MarketScan analysis 2005-2014. Cancers (Basel) 14: 1376, 2022.
5. Pallud J, Le Van Quyen M, Bielle F, Pellegrino C, Varlet P, Cresto N, Baulac M, Duyckaerts C, Kourdougli N, Chazal G, *et al*: Cortical GABAergic excitation contributes to epileptic activities around human glioma. Sci Transl Med 6: 244ra89, 2014.
6. Smoll NR, Gautschi OP, Schatlo B, Schaller K and Weber DC: Relative survival of patients with supratentorial low-grade gliomas. Neuro Oncol 14: 1062-1069, 2012.
7. Mistry M, Zhukova N, Merico D, Rakopoulos P, Krishnatry R, Shago M, Stavropoulos J, Alon N, Pole JD, Ray PN, *et al*: BRAF mutation and CDKN2A deletion define a clinically distinct subgroup of childhood secondary high-grade glioma. J Clin Oncol 33: 1015-1022, 2015.
8. Bell EH, Zhang P, Shaw EG, Buckner JC, Barger GR, Bullard DE, Mehta MP, Gilbert MR, Brown PD, Stelzer KJ, *et al*: Comprehensive genomic analysis in NRG oncology/RTOG 9802: A phase III trial of radiation versus radiation plus procarbazine, lomustine (CCNU), and vincristine in high-risk low-grade glioma. J Clin Oncol 38: 3407-3417, 2020.
9. Reuss DE, Sahm F, Schrimpf D, Wiestler B, Capper D, Koelsche C, Schweizer L, Korshunov A, Jones DT, Hovestadt V, *et al*: ATRX and IDH1-R132H immunohistochemistry with subsequent copy number analysis and IDH sequencing as a basis for an 'integrated' diagnostic approach for adult astrocytoma, oligodendroglioma and glioblastoma. Acta Neuropathol 129: 133-146, 2015.
10. Lise S, Clarkson Y, Perkins E, Kwasniewska A, Sadighi Akha E, Schnekenberg RP, Suminaite D, Hope J, Baker I, Gregory L, *et al*: Recessive mutations in SPTBN2 implicate β-III spectrin in both cognitive and motor development. PLoS Genet 8: e1003074, 2012.
11. Ikeda Y, Dick KA, Weatherspoon MR, Gincel D, Armbrust KR, Dalton JC, Stevanin G, Dürr A, Zühlke C, Bürk K, *et al*: Spectrin mutations cause spinocerebellar ataxia type 5. Nat Genet 38: 184-190, 2006.
12. Yang Z, Yu G, Guo M, Yu J, Zhang X and Wang J: CDPath: Cooperative driver pathways discovery using integer linear programming and Markov clustering. IEEE/ACM Trans Comput Biol Bioinform 18: 1384-1395, 2021.
13. Wu C, Dong B, Huang L, Liu Y, Ye G, Li S and Qi Y: SPTBN2, a new biomarker of lung adenocarcinoma. Front Oncol 11: 754290, 2021.
14. Huang M, Long Y, Jin Y, Ya W, Meng D, Qin T, Su L, Zhou W, Wu J, Huang C and Huang Q: Comprehensive analysis of the lncRNA-miRNA-mRNA regulatory network for bladder cancer. Transl Androl Urol 10: 1286-1301, 2021.
15. Wang P, Liu T, Zhao Z, Wang Z, Liu S and Yang X: SPTBN2 regulated by miR-424-5p promotes endometrial cancer progression via CLDN4/PI3K/AKT axis. Cell Death Dis 7: 382, 2021.
16. Feng P, Ge Z, Guo Z, Lin L and Yu Q: A comprehensive analysis of the downregulation of miRNA-1827 and its prognostic significance by targeting SPTBN2 and BCL2L1 in ovarian cancer. Front Mol Biosci 8: 687576, 2021.
17. Riesenberg S, Groetchen A, Siddaway R, Bald T, Reinhardt J, Smorra D, Kohlmeyer J, Renn M, Phung B, Aymans P, *et al*: MITF and c-Jun antagonism interconnects melanoma dedifferentiation with pro-inflammatory cytokine responsiveness and myeloid cell recruitment. Nat Commun 6: 8755-8755, 2015.
18. Brockmann L, Soukou S, Steglich B, Czarnewski P, Zhao L, Wende S, Bedke T, Ergen C, Manthey C, Agalioti T, *et al*: Molecular and functional heterogeneity of IL-10-producing $CD4^+$ T cells. Nat Commun 9: 5457, 2018.
19. Tang Z, Li C, Kang B, Gao G, Li C and Zhang Z: GEPIA: A web server for cancer and normal gene expression profiling and interactive analyses. Nucleic Acids Res 45: W98-W102, 2017.
20. Li JH, Liu S, Zhou H, Qu LH and Yang JH: starBase v2.0: Decoding miRNA-ceRNA, miRNA-ncRNA and protein-RNA interaction networks from large-scale CLIP-Seq data. Nucleic Acids Res 42: D92-D97, 2014.
21. Lyu X, Qiang Y, Zhang B, Xu W, Cui Y and Ma L: Identification of immuno-infiltrating MAP1A as a prognosis-related biomarker for bladder cancer and its ceRNA network construction. Front Oncol 12: 1016542, 2022.
22. Gregory AC, Zablocki O, Zayed AA, Howell A, Bolduc B and Sullivan MB: The gut virome database reveals age-dependent patterns of virome diversity in the human gut. Cell Host Microbe 28: 724-740 e8, 2020.

23. Zhang Y and Zhu J: Ten genes associated with MGMT promoter methylation predict the prognosis of patients with glioma. Oncol Rep 41: 908-916, 2019.
24. Hänzelmann S, Castelo R and Guinney J: GSVA: Gene set variation analysis for microarray and RNA-seq data. BMC Bioinformatics 14: 7, 2013.
25. Love MI, Huber W and Anders S: Moderated estimation of fold change and dispersion for RNA-seq data with DESeq2. Genome Biol 15: 550, 2014.
26. Chandrashekar DS, Bashel B, Balasubramanya SAH, Creighton CJ, Ponce-Rodriguez I, Chakravarthi BVSK and Varambally S: UALCAN: A portal for facilitating tumor subgroup gene expression and survival analyses. Neoplasia 19: 649-658, 2017.
27. Uhlen M, Oksvold P, Fagerberg L, Lundberg E, Jonasson K, Forsberg M, Zwahlen M, Kampf C, Wester K, Hober S, *et al*: Towards a knowledge-based human protein atlas. Nat Biotechnol 28: 1248-1250, 2010.
28. Wen PY and Packer RJ: The 2021 WHO classification of tumors of the central nervous system: Clinical implications. Neuro Oncol 23: 1215-1217, 2021.
29. World Health Organization (WHO): International Classification of Diseases (ICD). WHO, Geneva, 2022.
30. Salmena L, Poliseno L, Tay Y, Kats L and Pandolfi PP: A ceRNA hypothesis: The Rosetta stone of a hidden RNA language? Cell 146: 353-358, 2011.
31. Baumert BG, Hegi ME, van den Bent MJ, von Deimling A, Gorlia T, Hoang-Xuan K, Brandes AA, Kantor G, Taphoorn MJB, Hassel MB, *et al*: Temozolomide chemotherapy versus radiotherapy in high-risk low-grade glioma (EORTC 22033-26033): A randomised, open-label, phase 3 intergroup study. Lancet Oncol 17: 1521-1532, 2016.
32. Chatsirisupachai K, Lesluyes T, Paraoan L, Van Loo P and de Magalhães JP: An integrative analysis of the age-associated multi-omic landscape across cancers. Nat Commun 12: 2345-2345, 2021.
33. Wen JX, Li XQ and Chang Y: Signature gene identification of cancer occurrence and pattern recognition. J Comput Biol 25: 907-916, 2018.
34. Pignatti F, van den Bent M, Curran D, Debruyne C, Sylvester R, Therasse P, Afra D, Cornu P, Bolla M, Vecht C, *et al*: Prognostic factors for survival in adult patients with cerebral low-grade glioma. J Clin Oncol 20: 2076-2084, 2002.
35. Yue M, Liu T, Yan G, Luo X and Wang L: LINC01605, regulated by the EP300-SMYD2 complex, potentiates the binding between METTL3 and SPTBN2 in colorectal cancer. Cancer Cell Int 21: 504, 2021.
36. Xiao H, Bai J, Yan M, Ji K, Tian W, Liu D, Ning T, Liu X and Zou J: Discovery of 5-signature predicting survival of patients with lower-grade glioma. World Neurosurg 126: e765-e772, 2019.
37. Li Z, Zhu Z, Wang Y, Wang Y, Li W, Wang Z, Zhou X and Bao Y: has-miR-15a-5p inhibits colon cell carcinoma via targeting CCND1. Mol Med Rep 24: 735, 2021.
38. Qin S, He NB, Yan HL and Dong Y: Characterization of microRNA expression profiles in patients with giant cell tumor. Orthop Surg 8: 212-219, 2016.
39. Zhang J, Liu H, Hou L, Wang G, Zhang R, Huang Y, Chen X and Zhu J: Circular RNA_LARP4 inhibits cell proliferation and invasion of gastric cancer by sponging miR-424-5p and regulating LATS1 expression. Mol Cancer 16: 151, 2017.
40. Xu S, Tang L, Liu Z, Luo C and Cheng Q: Hypoxia-related lncRNA correlates with prognosis and immune microenvironment in lower-grade glioma. Front Immunol 12: 731048, 2021.
41. Li Y, Gao Y, Niu X, Tang M, Li J, Song B and Guan X: LncRNA BASP1-AS1 interacts with YBX1 to regulate Notch transcription and drives the malignancy of melanoma. Cancer Sci 112: 4526-4542, 2021.
42. Han X and Zhang S: Role of long non-coding RNA LINC00641 in cancer. Front Oncol 11: 829137, 2021.
43. Yang J, Yu D, Liu X, Changyong E and Yu S: LINC00641/miR-4262/NRGN axis confines cell proliferation in glioma. Cancer Biol Ther 21: 758-766, 2020.
44. Liao M, Liao W, Xu N, Li B, Liu F, Zhang S, Wang Y, Wang S, Zhu Y, Chen D, *et al*: LncRNA EPB41L4A-AS1 regulates glycolysis and glutaminolysis by mediating nucleolar translocation of HDAC2. EBioMedicine 41: 200-213, 2019.
45. Bin J, Nie S, Tang Z, Kang A, Fu Z, Hu Y, Liao Q, Xiong W, Zhou Y, Tang Y and Jiang J: Long noncoding RNA EPB41L4A-AS1 functions as an oncogene by regulating the Rho/ROCK pathway in colorectal cancer. J Cell Physiol 236: 523-535, 2021.
46. Cao Y and Aypar U: A novel Xq22.1 deletion in a male with multiple congenital abnormalities and respiratory failure. Eur J Med Genet 59: 274-277, 2016.
47. Petitprez F, Meylan M, de Reyniès A, Sautès-Fridman C and Fridman WH: The tumor microenvironment in the response to immune checkpoint blockade therapies. Front Immunol 11: 784, 2020.